RAPID COMMUNICATIONS

PHYSICAL REVIEW B VOLUME 45, NUMBER 14 1 APRIL 1992-II

Ostwald ripening in two and three dimensions

Jian Hua Yao, K. R. Elder, Hong Guo, and Martin Grant

Centre for the Physics of Materials, Physics Department, Rutherford Building, McGill University, 3600 rue University, Montréal, Québec, Canada H3A 2T8

(Received 2 October 1991; revised manuscript received 14 November 1991)

We present a new theoretical approach to Ostwald ripening of droplets for both two- and three-dimensional systems, where screening effects due to interacting droplets are incorporated. The solution of our mean-field equations gives both the coarsening rate and the droplet distribution function. The three-dimensional results conform well to experiments, while our two-dimensional results are in agreement with a numerical study we have performed.

When a binary mixture is cooled from the disordered phase into the two-phase metastable region (where the volume fraction ϕ of the minority component is small) the minority component condenses into spherical droplets. On average, the droplets grow in radius $R(t)$ as time goes on while their number decreases: large droplets grow by the condensation of material diffused through the matrix from small evaporating droplets. This phenomena is called Ostwald ripening. The classic theory for this is due to Lifshitz and Slyozov,[1,2] who studied the limit in which the volume fraction of the minority phase tends to zero, i.e., $\phi \rightarrow 0$. In an elegant calculation they determined the asymptotic growth rate of the droplets to be $\overline{R} = (Kt)^{1/3}$, where K is the coarsening rate, and the bar denotes an average. Furthermore, they found that the droplet distribution function obeyed the scaling form $f(R,t) = g(R/\overline{R})/\overline{R}^4$ for late times, and gave an expression for $g(z)$, the scaling function. These features, power-law growth and scaling, are now considered universal characteristics of the kinetics of a first-order phase transition.[3] The theory of Ostwald ripening by Lifshitz and Slyozov serves as an important example of this.

Nevertheless, it has proved difficult to rigorously test their theory by experiment or by numerical simulation. Experiments typically study volume fractions which are appreciably larger than zero, while numerical work has the additional problem of being practically difficult in three dimensions. Previous work on extending the theory of Lifshitz and Slyozov to nonzero ϕ has been attempted by many groups,[4–7] using both analytic and numerical methods. Nevertheless, this has remained a vexing problem in the field, for which a satisfactory resolution has not been found. The major analytical progress has been made by Marqusee and Ross,[4] and Tokuyama, Kawasaki, and Enomoto.[5] These theories give the form of the coarsening rate $K = K(\phi)$ and the scaling function $g = g(z,\phi)$ perturbatively in ϕ, predicting that K increases and g grows broader as the volume fraction increases. Unfortunately, these perturbation theories can neither go beyond $\mathcal{O}(\sqrt{\phi})$, nor be applied to two-dimensional systems. Furthermore, as we shall demonstrate below, so long as ϕ is greater than approximately 1%, the coarsening rate $K(\phi)$ and the droplet distribution function $g(z)$ are very sensitive to higher-order terms. For two-dimensional systems, a theory has been proposed by Marqusee,[8] which was extended and generalized by Zheng and Gunton.[9] However, Marqusee's two-dimensional theory is inconsistent with his three-dimensional theory with Ross, while Zheng and Gunton were not able to obtain a time-independent scaling distribution. Recently, Ardell[10] published an extension to two dimensions of his phenomenological theory for three-dimensional coarsening. His theory, unlike those mentioned above however, involves an *ad hoc*, although physically motivated free parameter.

We therefore felt it worthwhile to reinvestigate Ostwald ripening. The goal of this article is to present a systematic method to study Ostwald ripening in dimension $d = 2$ and $d = 3$, at nonzero volume fractions (for simplicity, ϕ will be called the volume fraction, although in $d = 2$ it is an area fraction). We use the same mean-field technique in both cases, and test our results by comparison to experiment and to a large-scale simulation study we have conducted.

Our study makes use of dimensionless variables. Units of length and time are given in terms of the capillary length $l_c = 2\gamma V_m/RT$ and a characteristic time $t^* = l_c^2/(DC_\infty V_m)$. These quantities involve the surface tension γ, the molar volume V_m, the gas constant R, the temperature T, the diffusion coefficient D, and the solute concentration in the matrix at a flat interface C_∞. It is also convenient to introduce a dimensionless concentration field $\theta(\mathbf{r}) = [C(\mathbf{r}) - C_\infty]/C_\infty$, where $C(\mathbf{r})$ is the concentration field at point $\mathbf{r}$ outside the droplets.

The many-droplet diffusion problem is intractable without approximation. In the steady-state limit, the fundamental equation is[6] $\nabla^2\theta(\mathbf{r}) = a\sum_{i=1}^{N} B_i\delta(\mathbf{r} - \mathbf{r}_i)$, where N is the number of the droplets in the system, $a = 2\pi^{d/2}/\Gamma(d/2)$, $\mathbf{r}_i$ gives the location of the ith droplet, and B_i gives the strength of the source of current for diffusion. This is the multiparticle diffusion equation in the quasistationary approximation. The δ functions on the right-hand side of the many-body diffusion equation result from the assumption that droplet locations remain fixed in the space and the distances among droplets

are much larger than the average droplet size. This is a very good description for systems with small volume fractions. The necessary boundary conditions are the Gibbs-Thomson condition for the concentration field at the curved surface of each droplet, and the imposed supersaturation far from all droplets, $\theta(\mathbf{r})|_{|\mathbf{r}-\mathbf{r}_i|=R_i} = 1/R_i$, for $i = 1, \ldots, N$, and $\lim_{r\to\infty} \theta(\mathbf{r}) = \theta_{\rm av}$, where $\theta_{\rm av}$ is the average concentration outside the droplets. The conservation law is $\sum_{i=1}^{N} B_i = 0$, while the growth law takes the form[6] $\dot{R}_i = B_i/R_i^{d-1}$.

Lifshitz and Slyozov made a mean-field approximation in the limit of $\phi \to 0$ to solve these equations. We shall make use of the fact that the steady-state problem resembles a homogeneous electron gas, since droplets interact via the the Laplace equation in the steady-state limit and the conservation law plays the role of charge neutrality. We introduce screening effects among the droplets and approximate many-droplet correlation effects in the same manner as the Thomas-Fermi mechanism for Coulomb systems. Based on a mean-field approximation, the growth law must obey

$$\frac{d(vR_i^d)}{dt} = I(R_i)[\theta_{\rm av} - \theta(R_i)], \tag{1}$$

where $v = \pi^{d/2}/\Gamma(d/2+1)$, assuming spherical growth. The mean-field approximation results from the assumption that the flux determining the growth rate for each droplet is only proportional to the difference between the boundary concentration and the *average* bulk concentration. The curvature-dependent rate coefficient $I(R)$ is unknown *a priori*, but will be determined self-consistently below. The continuity equation satisfies

$$\frac{\partial f(R,t)}{\partial t} + \frac{\partial}{\partial R}[\dot{R} f(R,t)] = 0. \tag{2}$$

The average bulk concentration field then obeys

$$\begin{aligned}\partial\theta_{\rm av}/\partial t &= -\partial \int f(R,t) v R^d dR/\partial t \\ &= -\int I(R)\theta_{\rm av} f(R,t) dR \\ &\quad + \int I(R)\theta(R) f(R,t) dR\end{aligned}$$

where we used Eqs. (1) and (2), integrating by parts. We now postulate an equation of motion for the local concentration field $\theta(\mathbf{r},t)$ near the ith droplet. The simplest form it can satisfy is $\partial\theta/\partial t = \nabla^2\theta - \xi^{-2}\theta + S - aB_i\delta(\mathbf{r}-\mathbf{r}_i)$. Herein, local diffusion is modified by the effective diffusion field from other droplets, giving rise to the screening length ξ and the background field $S\xi^2$. These quantities can be related to $I(R)$ by integrating the equation above and comparing with the time evolution of $\partial\theta_{\rm av}/\partial t$, giving $\xi^{-2} = \int I(R) f(R,t) dR$ and $S = \int I(R)\theta(R) f(R,t) dR$.

Equation (1) and the above one-body diffusion equation completely specify our mean-field approximation; indeed, they are the only approximations we make to solve the equations in the steady-state limit. In that limit, the concentration field obeys

$$\nabla^2\theta - \xi^{-2}\theta + \xi^{-2}\theta_{\rm av} = aB_i\delta(\mathbf{r}-\mathbf{r}_i) \tag{3}$$

near the ith droplet,[13] where we utilized the equation for the time evolution of $\partial\theta_{\rm av}/\partial t$. Applying the solution of Eq. (3) to the boundaries gives us $1/R_i = \theta_{\rm av} - B_i V(R_i/\xi)$ for $i = 1, \ldots, N$, where $V(R/\xi) = \exp(-R/\xi)/R$ for $d = 3$, $V(R/\xi) = K_0(R/\xi)$ for $d = 2$, and K_0 is a modified Bessel function. Substituting the solution B_i and $\theta_{\rm av}$ of the conservation law and the above boundary conditions into the growth law for the droplets' radii, we obtain

$$\frac{dR}{dt} = \frac{R^{1-d}}{V(R/\xi)}\left(\frac{\overline{[RV(R/\xi)]^{-1}}}{\overline{[V(R/\xi)]^{-1}}} - \frac{1}{R}\right). \tag{4}$$

Comparing this to Eq. (1) gives $I(R) = a/V(R/\xi)$, so that $\xi^{-2} = a\int[f(R,t)/V(R/\xi)]dR$.

From this point, Eqs. (2), (4), and the above ξ equation can be solved straightforwardly. First we note that the only scaling form $f(R,t)$ can satisfy is $f(R,t) = [\phi/\int_0^\infty z^d g(z)dz]g(z)/\overline{R}^{d+1}$ with $z = R/\overline{R}$, where f is normalized by the steady-state conservation law $\phi = \int dR v R^d f$. Making the convenient transformation $\xi = \eta\overline{R}$ and inserting the scaling form $f(R,t)$ into the ξ equation, we obtain $\eta^{-2} = \phi d\int g(z)/V(z/\eta)dz/\int z^d g(z)dz$. Using the scaling form $f(R,t)$ and substituting Eq. (4) into Eq. (2), we obtain a first-order separable partial differential equation. The solutions[13] are the following: $\overline{R} = [Kt + \overline{R}^3(t=0)]^{1/3}$ and $g(z) \propto [\exp\lambda d\int_0^z w^{-1}(z',\lambda)dz']/w(z,\lambda)$, where if $0 < z < z_o$, and $g(z) = 0$ otherwise, with $w(z,\lambda) = [z^{1-d}/V(z/\eta)](\sigma - z^{-1}) - \lambda z$ and

$$\sigma = \int_0^\infty \frac{g(z)}{zV(z/\eta)}dz \Big/ \int_0^\infty \frac{g(z)}{V(z/\eta)}dz,$$

where $w(z,\lambda)$ obeys $w(z_o,\lambda) = 0$ and $w'(z_o,\lambda) = 0$. Here λ is a time-independent separation factor, dependent upon ϕ and the coarsening rate K.

For vanishingly small ϕ, these equations can be solved analytically. In three dimensions, we recover the results of Lifshitz and Slyozov[1,2] for $\phi = 0$, while our leading-order in $\sqrt{\phi}$ corrections are identical to those calculated by Tokuyama, Kawasaki, and Enomoto.[5] Our two-dimensional results have the following form as $\phi \to 0$: $\overline{R} \sim [3t/(z_o^3 \ln\phi^{-1})]^{1/3}$, and $g(z) \propto z^2\exp\{2/[3(z/z_o)-3]\}/[(z_o-z)^{28/9}(z+2z_o)^{17/9}]$, if $0 < z < z_o = 1.406\,47$, and $g(z) = 0$ otherwise. These results differ from those of the theories for two dimensions due to Marqusee,[8] and Zheng and Gunton.[9] The logarithmic singularity in the growth rate implies that there is no consistent steady-state result for $d = 2$ when $\phi = 0$. In this regard, it should be noted that Rogers and Desai[12] obtained a *non*-steady-state result of $\overline{R} \sim (t/\ln t)^{1/3}$ in $d = 2$ for $\phi = 0$.

For larger values of ϕ (up to a limit discussed below), we numerically solved the $w(z_o,\lambda)$ equation self-consistently for z_o and λ in two and three dimensions. We first made a guess for σ and η, and then used the η and $w(z_o,\lambda)$ equations to compute new values of σ and η, repeating the procedure until consistent solutions were obtained.

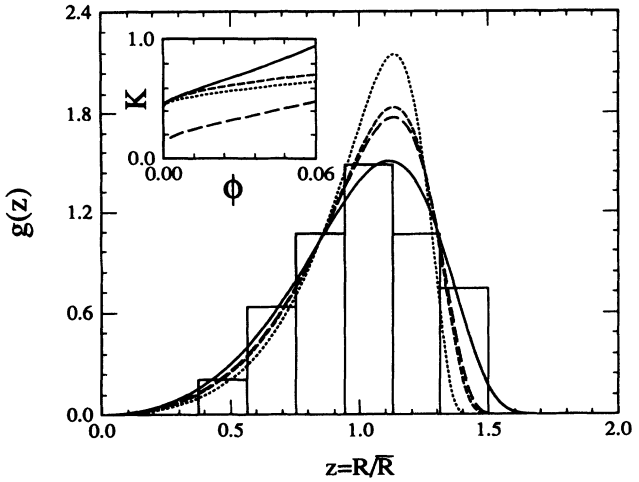

FIG. 1. Comparison of scaled normalized distribution functions $g(z)$ vs scaled droplet radius $z = R/\overline{R}$, from experiment and theory for $d = 3$. Histograms are the experimental distribution function at very late times (Ref. 11) for $\phi \sim 0.05$. Dotted, dashed, long-dashed, and solid lines are the respective predictions of Lifshitz and Slyozov ($\phi = 0$) (Ref. 1), Marqusee and Ross (Ref. 4), Tokuyama, Kawasaki, and Enomoto (Ref. 5), and us, for $\phi = 0.05$. The inset shows Coarsening rate $K(\phi)$ vs volume fraction ϕ. Dotted, dashed, and solid lines correspond, respectively, to the $d = 3$ results of Marqusee and Ross (Ref. 4), Tokuyama, Kawasaki, and Enomoto (Ref. 5), and us. The long-dashed line is our two-dimensional result.

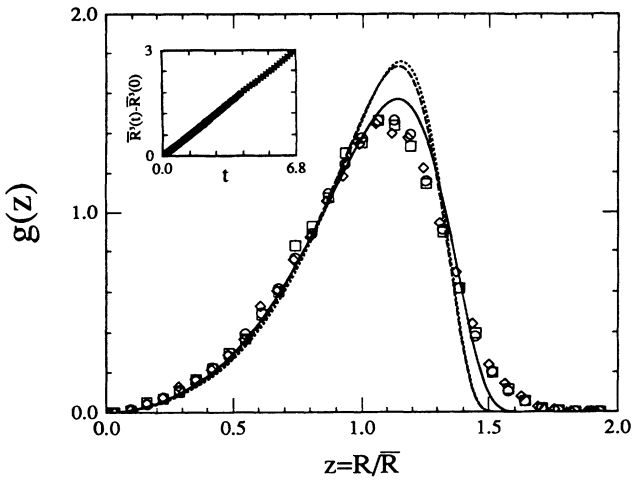

FIG. 2. Plot of the scaled normalized distribution function $g(z)$ vs the scaled radius $z = R/\overline{R}$ for $d = 2$. Dotted, dashed, and solid lines correspond, respectively, to Marqusee (Ref. 8), Ardell (Ref. 10), and us for $\phi = 0.05$. Circles, squares, and triangles give the scaled normalized distribution functions from the simulation, corresponding, respectively, to the number of remaining droplets being $N \simeq 500$, 400, and 300, for $\phi = 0.05$. The inset shows the simulation result for growth law $\overline{R} = [Kt + \overline{R}^3(t = 0)]^{1/3}$, with $K = 0.447$. Both axes of the inset are scaled by 10^{-7}.

Figure 1 shows the theoretical predictions for the scaled and normalized distribution functions, as well as experimental results[11] for $d = 3$. Our prediction is in good agreement with the experimental results, although those results do not provide a strong test for theory. In the inset we show the relation between the coarsening rate K and the volume fraction ϕ. Our theory predicts that the coarsening rate is very sensitive to the volume fraction ϕ for both two- and three-dimensional systems. One can also see that high-order volume fraction effects are very important for the K: for example, the inset shows that, for $\phi > 0.01$, the perturbatively calculated coarsening rate of Tokuyama, Kawasaki, and Enomoto differs significantly from ours.

Our theory is inapplicable to large volume fractions where the screening length ξ is close to the average radius of the droplets $\overline{R}$, since we make a Thomas-Fermi approximation and treat the droplets as point sources and sinks. Indeed, there is no solution for ξ, $g(z)$, and $w(z_o, \lambda)$ equations if $\xi < 2.7\overline{R}$ for $d = 2$ and $\xi < 1.9\overline{R}$ for $d = 3$, corresponding to $\phi > 0.085$ and $\phi > 0.06$, respectively. This gives self-consistent criteria for the applicability of our approach.

To test our predictions for two dimensions, we have undertaken a numerical simulation, similar to that of Voorhees and Glicksman.[6] We used Ewald's technique[6] and applied the solution of the many-body diffusion equation to the Gibbs-Thomson boundary condition to obtain[13]

$$\frac{1}{R_j} = B_o - \frac{2\pi}{L^2}\sum_{i=1}^{N} B_i \sum_{\mathbf{k}\neq 0} \frac{e^{-k^2/4L^2}}{k^2} e^{i\mathbf{k}\cdot\mathbf{r}_{ij}} + B_j[\ln(R_j/L) + b] - \sum_{i\neq j}^{N} B_i E_1(r_{ij}/L), \quad (5)$$

where L is the system size, B_o is a nonzero constant,

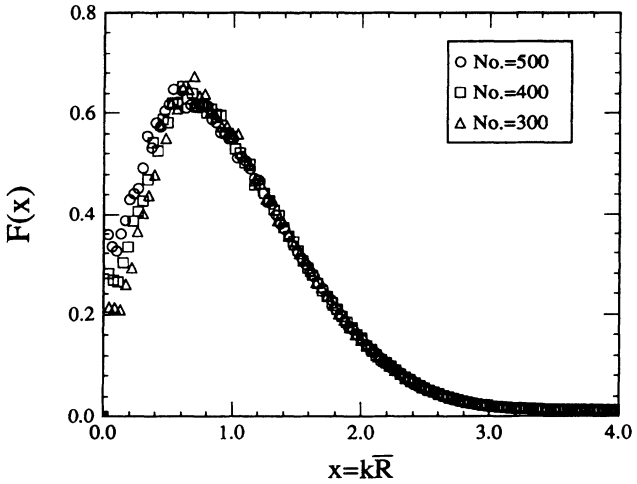

FIG. 3. Scaled structure factor $F(x)$ vs dimensionless wave number $x = k\overline{R}$, in $d = 2$. Circles, squares, and triangles give the scaled normalized distribution functions from the simulation, corresponding, respectively, to the number of remaining droplets being $N \simeq 500$, 400, and 300.

$b = \int_0^{\infty} dr'(1-e^{-r'/\bar{l}})/r' - E_1(1)$, $\mathbf{r}_{ij} = \mathbf{r}_i - \mathbf{r}_j$, and $E_1(x) = \int_x^{\infty} dt\, e^{-t}/t$.

The growth law for R, the conservation law for B_i, and Eq. (5) are the basic equations of our simulations. The system was inisialized by randomly generating a set of $\{R_i\}$ consistent with the distribution function of our analytical calculation, the solid line in Fig. 2, and randomly placing the droplets in the available space without overlap. We also used other initial conditions, and found that the distribution function approached the same limiting form, for a given volume fraction. After setting the initial radii and locations of the droplets, solving Eq. (5) with the conservation law for B_i gives a set of $\{B_i\}$. Then, substituting the set of $\{B_i\}$ into the growth law gives a new set of $\{R_i\}$, and so on. We used toroidal boundary conditions and averaged over 50 independent sets of initial conditions.

Typically, systems with 1000 droplets were studied. The evolution of the system was followed until the total number of droplets was reduced to approximately 300. Figure 2 is a plot of a scaled and normalized distribution function. The data collapse of the simulation results confirms the scaling relation $f(R,t) \propto g(R/\overline{R})/\overline{R}^{d+1}$. The inset shows that the average radius complies with $\overline{R} = [Kt + \overline{R}^3(t=0)]^{1/3}$, and is consistent with our analytic solution for $\overline{R}$, where the numerical simulations give $K = 0.447$.

The solid line is the distribution function of our analytic calculations for $\phi = 0.05$; the dotted and dashed lines give, respectively, the results of Marqusee[8] and Ardell.[10] Ardell's work, unlike our theory or Marqusee's, involves a free parameter.[14] Therefore, in our comparison, we have fixed this parameter by letting the coarsening rate K in his theory equal the numerically observed rate. Marqusee's theory, with no free parameters, gives a coarsening rate of $K = 0.373$, as compared to our numerical result of 0.447 and our analytic result (which also involves no free parameters) of 0.436. Overall, our theoretical predictions for $g(z)$ and K compare very well to the numerical simulation.

We expect other quantities than the distribution function to exhibit scaling. For example, the structure factor, $s(\mathbf{k},t) = \overline{|\delta\theta(\mathbf{k},t)|^2}$, where $\delta\theta$ is the deviation of θ from its average value, and k is the wave number, should satisfy a scaling form.[3] Namely, $S(k,t) = \sum_{\hat{k}} s(\mathbf{k},t)/\sum_{\hat{k}} 1 = \overline{R}^d F(k\overline{R})$, where the sum $\sum_{\hat{k}}$ is over a spherical shell defined by $n - \frac{1}{2} \le |\mathbf{k}|L/(2\pi) < n + \frac{1}{2}$ and the grid is $L^2 = 512^2$. This is an important quantity, which can be estimated directly by many experimental methods, although we note again that our results for $S(k,t)$ are for two dimensions. Figure 3 shows a plot of the scaled structure factor where all data collapses approximately to a single universal curve, as expected. A similar shape for the two-dimensional scaling function for small ϕ has been reported recently by Chakrabarti, Toral, and Gunton,[15] who numerically solved the Langevin equation of model B.

We thank Zaven Altounian for helpful discussions. This work was supported by the Natural Sciences and Engineering Research Council of Canada, and les Fonds pour la Formation de Chercheurs et l'Aide à la Recherche de la Province du Québec.

[1] I. M. Lifshitz and V. V. Slyozov, J. Phys. Chem. Solids **19**, 35 (1961).

[2] C. Wagner, Z. Electrochem. **65**, 581 (1961).

[3] J. D. Gunton, M. San Miguel, and P. S. Sahni, in *Phase Transitions and Critical Phenomena*, edited by C. Domb and J. L. Lebowitz (Academic, London, 1983), Vol. 8.

[4] J. A. Marqusee and J. Ross, J. Chem. Phys. **80**, 536 (1984).

[5] M. Tokuyama and K. Kawasaki, Physica **123A**, 386 (1984); K. Kawasaki and Y. Enomoto, *ibid.* **134A**, 323 (1986); **135A**, 426 (1986); Y. Enomoto, M. Tokuyama, and K. Kawasaki, Acta Metall. **34**, 2119 (1986).

[6] P. W. Voorhees and M. E. Glicksman, Acta Metall. **32**, 2001 (1984); **32**, 2013 (1984); P. W. Voorhees, J. Stat. Phys. **38**, 231 (1985); P. P. Ewald, Ann. Phys. (Leipzig) **64**, 253 (1921).

[7] M. Marder, Phys. Rev. Lett. **55**, 2953 (1985); Phys. Rev. A **36**, 858 (1987).

[8] J.A. Marqusee, J. Chem. Phys. **81**, 976 (1984).

[9] Q. Zheng and J.D. Gunton, Phys. Rev. **A 39**, 4848 (1989).

[10] A. J. Ardell, Phys. Rev. B **41**, 2554 (1990); Acta Metall. **20**, 61 (1972).

[11] K. Rastogi and A.J. Ardell, Acta Metall. **19**, 321 (1971).

[12] T. M. Rogers and R. C. Desai, Phys. Rev. B **39**, 11 956 (1989).

[13] Further results will be given in a future paper: J. H. Yao, K. R. Elder, H. Guo, and M. Grant (unpublished).

[14] The free parameter in Ardell's theory arises from a physically motivated, but *ad hoc* cutoff for steady-state diffusion. He mimics finite volume fraction effects via the cutoff length $r' = R + \beta\bar{l}$, where $\bar{l}$ is the mean distance between a droplet and its nearest neighbor and so is determined by the volume fraction, R is the radius of an average droplet, and β is a number set by Ardell to $\frac{1}{2}$. He notes that this choice is arbitrary (Ref. 10), so we have simply fixed β by fitting K as mentioned above. Alternatively, if we fit Ardell's distribution as best as possible to the numerically observed one, the coarsening rate from that theory is too large by a factor of 3.

[15] A. Chakrabarti, R. Toral, and J. D. Gunton (unpublished).